



Root electrotropism in *Arabidopsis* does not depend on auxin distribution but requires cytokinin biosynthesis

Maddalena Salvalaio,¹ Nicholas Oliver,^{1,†} Deniz Tknaz,¹ Maximillian Schwarze ,^{1,†} Nicolas Kral,^{1,†} Soo-Jeong Kim^{1,†} and Giovanni Sena ,^{1,*,#}

¹ Department of Life Sciences, Imperial College London, London SW7 2AZ, UK

*Author for communication: g.sena@imperial.ac.uk

†Present addresses:

Nicholas Oliver, Department of Physics, Freie Universität Berlin, Berlin 14195, Germany.

Maximillian Schwarze, School of Biosciences, University of Birmingham, Birmingham B15 2TT, UK.

Nicolas Kral, Phytoform Labs Ltd., Lawes Open Innovation Hub, Harpenden, Harpenden AL5 2JQ, UK.

Soo-Jeong Kim, Department of Engineering, University of Cambridge, Cambridge CB2 1TN, UK.

#Senior author.

M.Sa., N.O., and G.S. conceived and designed the experiments. M.Sa. contributed to the development of the V-box, and performed and analyzed most of the electrotropism assays. N.O. contributed to the development of the V-box, and performed and analyzed some of the WT electrotropism assays. D.T. contributed to the development of the V-slide and performed some of the electrotropism assays. M.Sc. performed the root excision experiments and the electrotropism assays for *cyp735a1*, and analyzed the data. N.K. contributed to the development of the V-slide and performed the *R2D2* and *WAVE131Y* imaging. S.-J.K. performed the heat-treatment experiments. M.Sa. and G.S. prepared the manuscript, with all the authors contributing to the “Materials and methods.”

The author responsible for distribution of materials integral to the findings presented in this article in accordance with the policy described in the Instructions for Authors (<https://academic.oup.com/plphys/pages/General-Instructions>) is: Giovanni Sena (g.sena@imperial.ac.uk).

Abstract

Efficient foraging by plant roots relies on the ability to sense multiple physical and chemical cues in soil and to reorient growth accordingly (tropism). Root tropisms range from sensing gravity (gravitropism), light (phototropism), water (hydrotropism), touch (thigmotropism), and more. Electrootropism, also known as galvanotropism, is the phenomenon of aligning growth with external electric fields and currents. Although root electrotropism has been observed in a few species since the end of the 19th century, its molecular and physical mechanisms remain elusive, limiting its comparison with the more well-defined sensing pathways in plants. Here, we provide a quantitative and molecular characterization of root electrotropism in the model system *Arabidopsis* (*Arabidopsis thaliana*), showing that it does not depend on an asymmetric distribution of the plant hormone auxin, but instead requires the biosynthesis of a second hormone, cytokinin. We also show that the dose–response kinetics of the early steps of root electrotropism follows a power law analogous to the one observed in some physiological reactions in animals. Future studies involving more extensive molecular and quantitative characterization of root electrotropism would represent a step toward a better understanding of signal integration in plants and would also serve as an independent outgroup for comparative analysis of electroreception in animals and fungi.

Introduction

Plant roots navigate the complex soil environment in search of water and nutrients through various sensing mechanisms reorienting their growth toward or away from signal sources (tropism) (Muthert et al., 2020). For example, hydrotropism redirects growth toward high moisture (Miyazawa and Takahashi, 2019), (negative) phototropism redirects away from light sources (Kutschera and Briggs, 2012), and gravitropism induces growth downward, following the gravity vector (Su et al., 2017). The integration of overlapping and frequently contradicting molecular and physical signals is as critical for plant roots as it is for other soil organisms.

Although many molecular aspects of a few root tropisms have been understood (Muthert et al., 2020), several key sensing mechanisms remain elusive. One of these is the capacity of plant roots to sense electric fields (electrotropism or galvanotropism) (Navez, 1927). The local physical and chemical properties of soil determine the presence of mobile electrical charges and the generation of spontaneous electric fields (Pozdnyakov and Pozdnyakova, 2002). For example, electrostatic fields can appear from charge separation in minerals like clay (Ward, 1990), by electrokinetic conversion caused by a conducting fluid like water flowing through rocks (Revil et al., 2003) or by local accumulation of mineral ions important for plant metabolism such as ammonium and nitrate ions. Local electric fields in soil can have biological origins as well, for example, from negatively charged bacteria (Olitzki, 1932) or from ions and charged molecules released by microorganisms (Chabert et al., 2015) or plant roots (Takamura, 2006). All this suggests that transient electrostatic fields in soil encode unique information regarding the localization of water, micronutrients, and organisms, and it is plausible that a sensing mechanism to detect such signal provides a selective advantage.

In fact, the reception of electric fields (electroreception) has been observed in vertebrates (Crampton, 2019) and invertebrates (Clarke et al., 2013), including common model systems such as *Caenorhabditis elegans* (Sukul and Croll, 1978) and *Dictyostelium* (Shanley et al., 2006), as well as in fungi (McGillivray and Gow, 1986). Interestingly, electric sensing structures have been identified only in a few aquatic animal species (Peters et al., 2007) and more recently in bumblebees (Sutton et al., 2016).

First recorded in 1882 (Elfving 1882) and rediscovered at the start of the 20th century (Ewart and Bayliss, 1905), root electrotopism has been studied sporadically in maize (*Zea mays*), peas (*Pisum sativum*), and bean (*Vigna mungo*) but with contradicting results (Wolverton et al., 2000). Crucially, the anatomical and molecular details of sensing electric fields are still largely unknown in roots. A quantitative description of root electrotopism's kinetics is also missing, preventing a comparative analysis with animal electroreception and electrotaxis.

Results

Developing a root electrotopism assay

To study root electrotopism in the plant model system *Arabidopsis* (*Arabidopsis thaliana*), we developed a setup to

stimulate, image, and quantitate electrotopism in its primary root. Briefly, roots were grown vertically in a transparent chamber (V-box) containing a buffered liquid medium and two immersed electrodes connected to a power supply to generate a uniform electric field and an ionic current perpendicular to the growing roots (Figure 1, a and “Materials and methods”).

To maintain a constant temperature and minimize the pH gradient generated by electrolysis, the liquid medium was continuously circulated in a closed loop between the V-box, a cooled water bath and a 2-L reservoir bottle (Supplemental Figure S1 and “Materials and methods”). In each V-box, the primary roots of five seedlings were imaged every 10 min with a camera mounted in front of the V-box (Supplemental Figure S1 and “Materials and methods”). We measured the actual field generated in the medium by immersing voltmeter probes in the two neighboring positions of each seedling: as expected, the field measured in the medium was lower than the nominal imposed in air between the two electrodes, but still relatively uniform across the five positions (Supplemental Figure S2, a). At the same time, we measured the current passing through the circuit (Supplemental Figure S2, b and “Materials and methods”).

To quantify the root response to the applied electric field, we took an image of the roots every 10 min and measured the angle between the root tip and the vertical gravity vector (Figure 1, b).

To confirm that the circulation of the liquid medium was effective in damping any pH gradient created by electrolysis and in eliminating any chemotropic effect, we imposed a field of 1.5 V/cm in a V-box without plants for 1 h while maintaining liquid circulation. We then turned off the field and the liquid circulation, immediately positioned the plants in the V-box, and imaged the roots for the next 80 min: we did not observe any significant deviation in root growth direction (t test between 1.5 and 0 V/cm at 80 min, $P = 0.859$), compared with roots in a V-box that never experienced the electric field (Supplemental Figure S2, c), indicating that no significant pH gradient was left in the medium.

Root tip reorientation in external electric fields

We measured the response of wild-type (WT) *Arabidopsis* primary roots to a continuous electric field. The distribution of reorientations to a range of field intensities between 0.5 and 2.5 V/cm shows a quick tropism toward the negative electrode, or cathode (Figure 1, c).

We wondered how much of this effect was due to trivial electrostatic, that is, the physical pull toward the negative electrode due to a hypothetical net positive charge accumulated on the root tip, rather than a more complex biological response involving molecular signaling. To address this, we deactivated the roots by immersing them in a 50°C bath for 10 min, until growth and gravitropism were suppressed (0/9 roots growing and bending to gravity after exposure to 50°C, versus 10/10 after exposure to 23°C), transferred to the V-box and exposed them to a 2.0 V/cm electric field: the root response shows that this simple treatment was

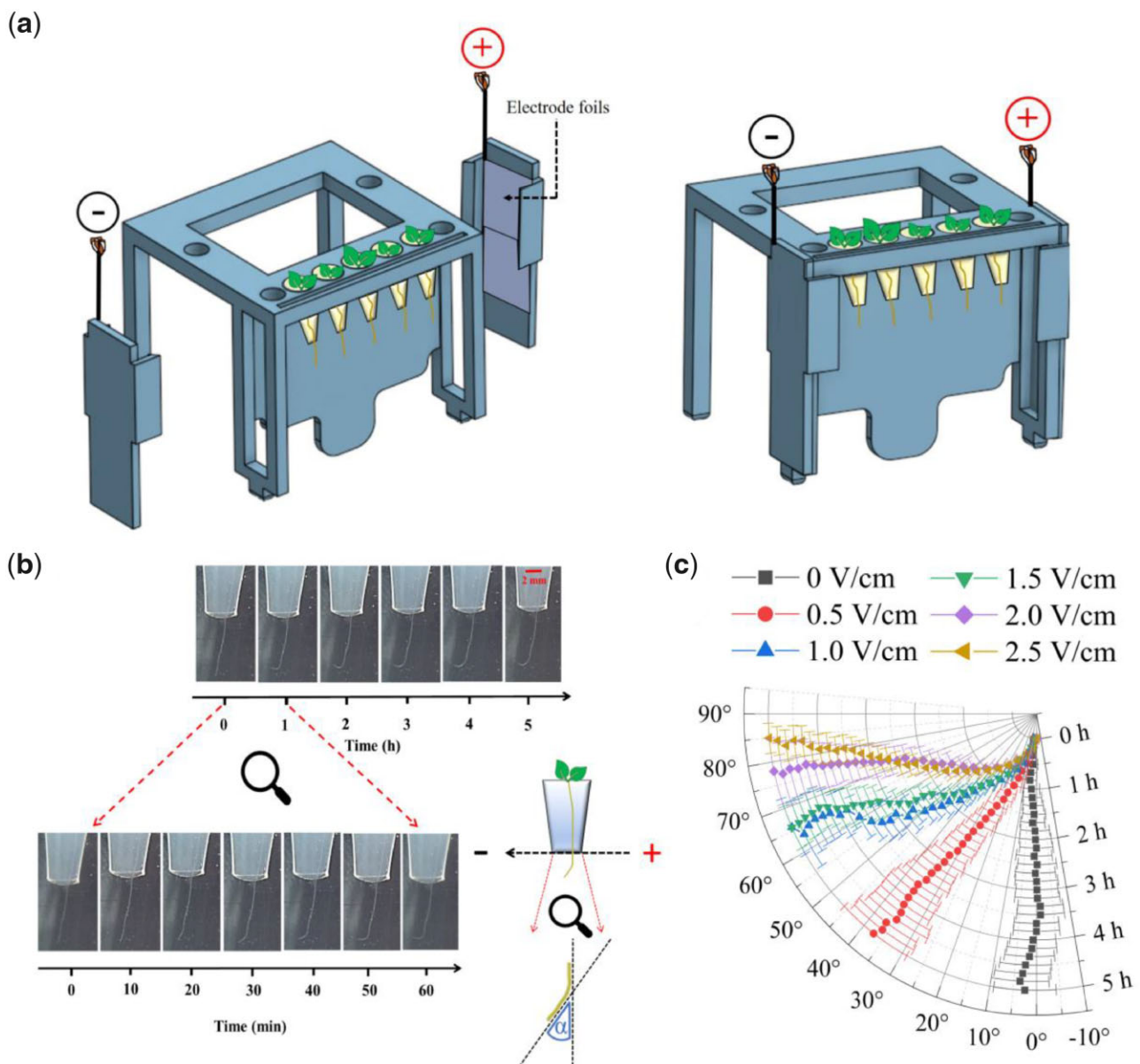


Figure 1 Arabidopsis root electrotopism. a, Schematic of the 3D-printed module used in the V-box. b, Representative time-lapse series of a single root as imaged by the Raspberry camera from the V-box; inset, schematic of the angle measured. c, Polar plot of the average root tip orientations relative to the gravity vector, with time on the radial axis and orientation angle on the circumferential axis; 0 V/cm, $N = 10$; 0.5 V/cm, $N = 9$; 1.0 V/cm, $N = 8$; 1.5 V/cm, $N = 21$; 2.0 V/cm, $N = 18$; 2.5 V/cm, $N = 20$. Error bars, s.e.m.

sufficient to completely inhibit electrotopism when compared with roots kept at a standard 23°C temperature (t test between 50°C and 23°C at 5 h, $P < 0.001$), strongly suggesting that electrostatic alone could not explain the root response and that this is in fact a biological phenomenon (Supplemental Figure S3).

Response curves

The progressively sharper root tip reorientation as the field intensity was increased (Figure 1, c) suggests that the sensing mechanism is not acting as a simple on/off switch but that it can distinguish electric fields of different strengths.

To quantitate this, we plotted the orientation angle at 5 h (“response”) as a function of the electric field intensity (“stimulus”) and found a best fit with a power function with exponent 0.45 (Figure 2, a, left), indicating that the resolution of the sensor is higher at low-intensity stimuli (steep response curve) than at high-intensity stimuli (shallow response curve). The analogous response curve as a function of the measured current intensity is best fit with a power function with exponent 0.33 (Figure 2, a, right).

Since the root tip reorientations did not show any obvious overshoot (Figure 1, c), we looked more closely at the angular velocity: the maximum average velocity in WT roots

was reached when the root tip was oriented between 10 and 20 degrees to the gravity vector and then progressively decreased as the root tip approached its maximum reorientation (Supplemental Figure S4, a). This indicates that the mechanism is able to sense and respond differently to the changing relative orientation of the tip with the external electric field and to progressively slow down the root tip rotation as it approaches the target orientation. Moreover, the maximum angular velocity appears to be roughly proportional to the electric field strength (Figure 2, b, left), although this is much less evident as a function of the electric current (Figure 2, b, right).

Root tips are not damaged

Early reports noted that protracted exposure to external fields could cause physical damage to plant root tips (Wawrecki and Zagórska-Marek, 2007). To control whether this was the case in our experimental conditions, we developed a simple chambered slide (V-slide) to be mounted on a standard confocal microscope stage (Supplemental Figure S5, a and “Materials and methods”)

with electrodes on the chamber’s sides and a circulating liquid medium for temperature control similar to the one implemented in the V-box (Supplemental Figure S5, b). Seedlings from the Arabidopsis transgenic line constitutively expressing the yellow fluorescent cell-membrane marker WAVE 131Y (Geldner et al., 2009) were mounted on the V-slide and imaged at cellular resolution while exposed to a 1.0 V/cm electric field (“Materials and methods”). The field of view in our time-lapse images comprises the meristem, the transition zone, and the distal elongation zone, but no cellular pattern perturbation was noticeable in any of these regions when compared with roots not exposed to the field (Supplemental Figure S6). Also, the time lapse suggests that asymmetric cell expansion in the elongation zone is causing the bending, as expected from other examples of root tropism (Gilroy, 2008).

To further confirm that roots exposed to the electric field are not damaged and maintain gravitropic response, we monitored root tips for 2 h after the electric field had been turned off, observing a clear gravitropic behavior (Supplemental Figure S7).

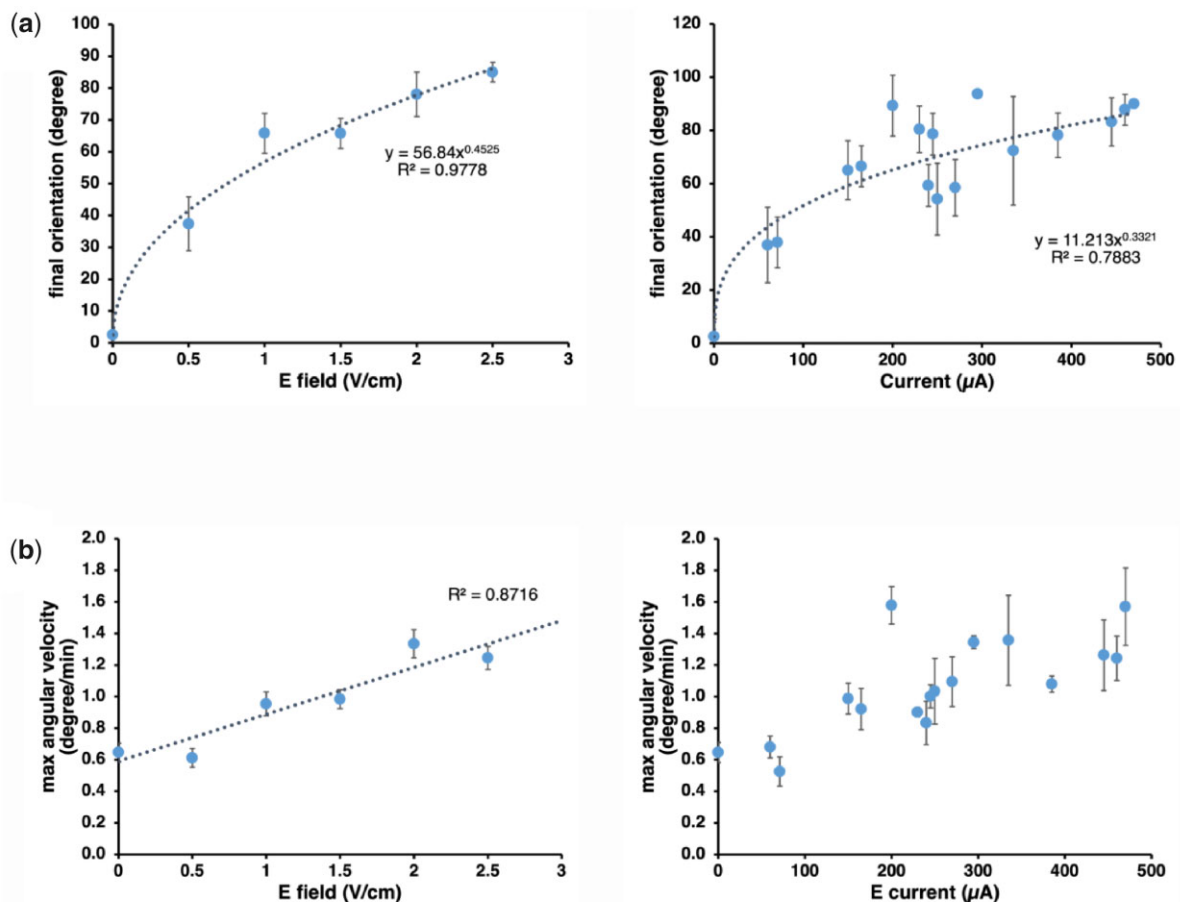


Figure 2 Root electrotropism dynamics. a, Root electrotropism response curves: average root tip orientations after 5 h of exposure to a given electric field (left panel; $N = 86$) or current (right panel; $N = 75$); error bars, s.e.m.; R^2 , coefficient of determination. b, Average maximum angular velocity reached by the root tip after 5 h of exposure to a given electric field (left panel; $N = 86$) or current (right panel; $N = 75$). Error bars, s.e.m.; R^2 , coefficient of determination.

Regions of competence

Since the root bending occurs in the elongation zone, we wanted to identify the region responsible for sensing the electric field. We excised distal fragments of the root at 125, 300, 400, and 500 μm from the tip (Figure 3, a), and then exposed the cut root to 1.5 V/cm (“Materials and methods”).

In the first 2 h (Figure 3, b, left), roots cut at 400 μm from the tip turned to angles indistinguishable from uncut roots exposed to the same field (Wilcoxon between 400 μm cut and uncut at 1.5 V/cm at 2 h, $P = 0.211$), while roots cut at 500 μm from the tip did not turn and at 2 h showed orientations indistinguishable from uncut roots not exposed to a field (t test between 500 μm cut at 1.5 V/cm and uncut at 0 V/cm at 2 h, $P = 0.164$). These results indicate that the 400 μm distal fragment is not necessary for the early (2 h) electrotopical response, while the 500 μm distal fragment is; since the elongation zone involved in the bending spans an extended region proximal to the 500 μm cut, we conclude that in *Arabidopsis* roots the region between 400 and 500 μm from the tip is necessary for early sensing an external electric field.

Between 2 and 5 h of exposure (Figure 3, b, right), while roots cut at 300 μm on average continue to turn like the uncut roots (t test between 300 μm cut and uncut at 1.5 V/cm at 5 h, $P = 0.071$), roots cut at 400 μm quickly fail to sustain their response and at 5 h they show tip orientations on average different than those of uncut roots exposed to the same field (t test between 400 μm cut and uncut at 1.5 V/cm at 5 h, $P < 0.001$). These results indicate that the 300 μm distal fragment is not necessary to maintain the electrotopical response up to 5 h, while the 400 μm distal fragment is; we conclude that in *Arabidopsis* roots the region between 300 and 400 μm from the tip is necessary for prolonged sensing of the imposed electric field.

Interestingly, previous studies suggested that the movement of Ca^{++} ions accumulated in the mucilage at the very tip of the root might be involved in electrotopical sensing (Marcum and Moore, 1990). Since any excision above

125 μm from the tip is likely to remove most of the mucilage from the root, our results don't seem to support this hypothesis.

Auxin distribution is not altered by the electric field

The fact that roots without tips could still respond to the electric field shows that even a major disruption of the stereotypical auxin redistribution mechanism is not sufficient to inhibit electrotopism.

On the other hand, an asymmetric accumulation of auxin is required for asymmetric cell elongation and root bending in some tropisms, as suggested by the classic Cholodny–Went model (Thimann and Went, 1937). To test whether this model applied to electrotopism, and whether the external electric field is sufficient to induce an asymmetric distribution of auxin in the root, we exposed roots expressing the auxin-sensitive fluorescent reporter *R2D2* (Liao et al., 2015) to a field of 1.0 V/cm for 30 min, before quickly mounting them on a microscope slide and imaging them with a confocal microscope (“Materials and methods”). A ratiometric quantification of *R2D2* signal (Kral et al., 2016) in each epidermal cell (Figure 4, a and “Materials and methods”) showed that the average auxin response measured in the epidermal cells on the side facing the negative electrode and on the side facing the positive electrode was statistically indistinguishable (Figure 4, b; “Materials and methods”), both in the distal (Wilcoxon test, $P = 0.696$) and the proximal (Wilcoxon test, $P = 0.843$) region of the root, indicating that auxin is not asymmetrically distributed after exposure to the electric field.

Moreover, both sides were also indistinguishable from the average between the two sides in roots not exposed to the field (mock), both in the distal (Wilcoxon test between the negative exposed side and mock, $P = 0.775$ and between the positive exposed side and mock, $P = 0.881$) and in the proximal (Wilcoxon test between the negative exposed side and mock, $P = 0.041$ and between the positive exposed side and mock, $P = 0.098$) regions.

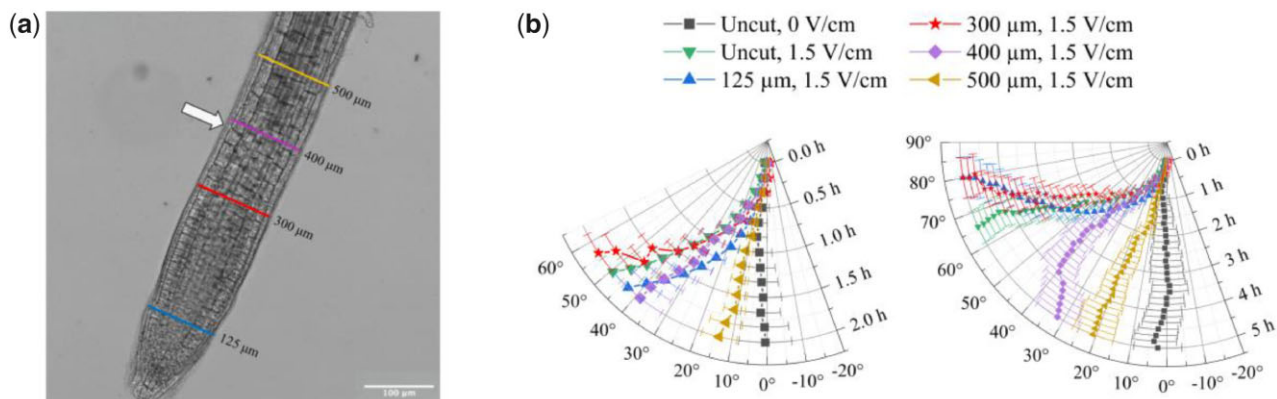


Figure 3 Electrotopism of decapitated roots. a, Points of excision overlapped to a representative microscope image of the *Arabidopsis* primary root tip; arrow, transition point; scale bar, 100 μm . b, Polar plot of the average root tip orientations relative to the gravity vector, with time on the radial axis and orientation angle on the circumferential axis; the same data are presented for the first 2 h (left panel) and for the full 5 h (right panel); Uncut at 0 V/cm, $N = 10$; Uncut at 1.5 V/cm, $N = 21$; 125 μm , $N = 16$; 300 μm , $N = 7$; 400 μm , $N = 10$; 500 μm , $N = 10$. Error bars, s.e.m.

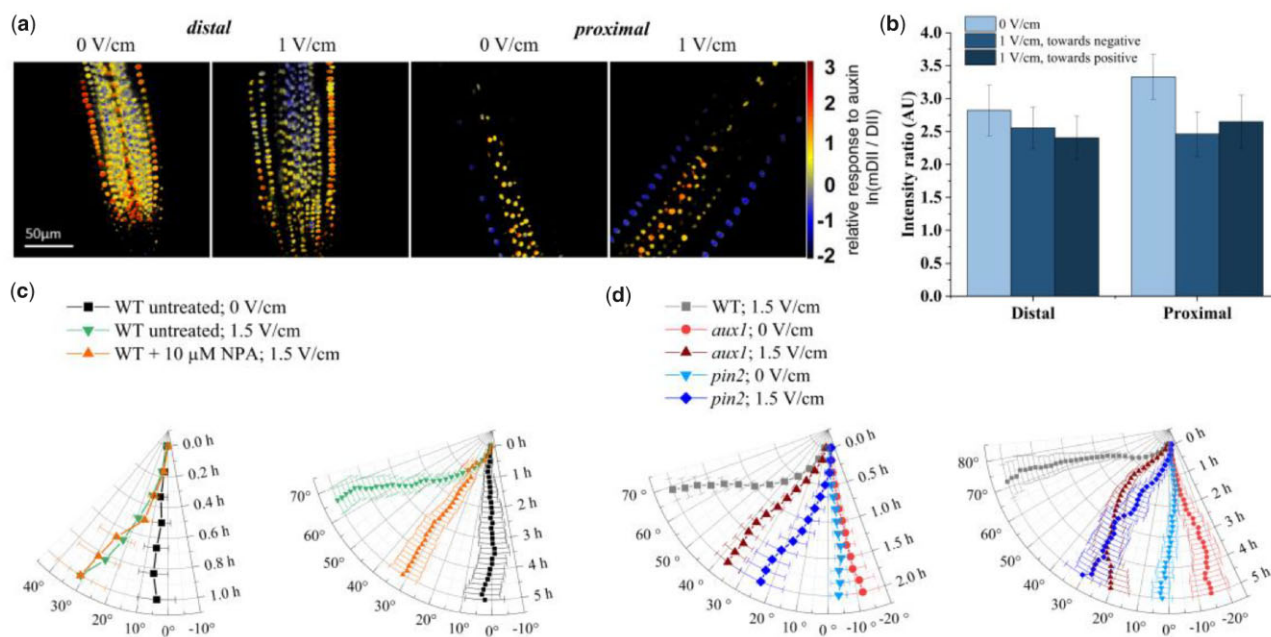


Figure 4 Auxin distribution. a, Relative response to auxin concentration in Arabidopsis primary root tips, indicated by the ratiometric fluorescent reporter *R2D2* (see “Materials and methods”); left panels: representative tip (distal) regions at 0 and 1 V/cm; right panels: representative higher (proximal) regions at 0 and 1 V/cm; scale bar, 50 μm (valid for all panels). b, Quantification of the average relative response to auxin (as shown in a) in the epidermis cell layer facing the positive or negative electrode, in the distal and proximal regions; the data for 0 V/cm are an average between the two sides; error bars, s.e.m. c and d, Polar plots of the average root tip orientation relative to the gravity vector, with time on the radial axis and orientation angle on the circumferential axis: c, NPA treatment; the same data are presented for the first 1 h (left panel) and for the full 5 h (right panel); untreated at 0 V/cm, $N = 10$; untreated at 1.5 V/cm, $N = 21$; 10 μM , $N = 21$. d, *aux1* (0 V/cm, $N = 14$; 1.5 V/cm, $N = 18$) and *pin2* (0 V/cm, $N = 13$; 1.5 V/cm, $N = 13$) mutants; WT at 1.5 V/cm, $N = 15$; the same data are presented for the first 2 h (left panel) and for the full 5 h (right panel). Error bars, s.e.m.

Auxin transport is not necessary for early response

Previous work indicated that auxin transport inhibitors can inhibit electrotopism response in maize roots (Ishikawa and Evans, 1990). To verify this in Arabidopsis, and further explore the role of auxin in root electrotopism, we used *N*-1-naphthylphthalamic acid (NPA) to inhibit polar auxin transport (Sabatini et al., 1999) while exposing the roots to the electric field. We tested 0.1, 1.0, and 10 μM NPA and found that 10 μM NPA was the lowest concentration of NPA to inhibit gravitropism (“Materials and methods”), a known auxin-dependent tropism.

We pre-treated the seedlings for 3 h in liquid medium containing 10 μM NPA (“Materials and methods”) and then transferred them to a V-box containing 10 μM NPA in the medium and the reservoir. In the first 1 h of field exposure (Figure 4, c, left) the NPA-treated roots reoriented at angles indistinguishable from those of untreated ones (Wilcoxon test between NPA-treated and untreated at 1 h, $P = 0.350$). From 1 to 5 h of exposure (Figure 4, c, right), NPA-treated roots respond less than the untreated (t test between NPA-treated and untreated at 5 h, $P < 0.001$), but still significantly more than the untreated and those not exposed to the field (t test between untreated at 1.5 and 0 V/cm at 5 h, $P = 0.001$). These results indicate that auxin polar transport is not necessary for an early electrotopism response but might play a role in maintaining a long-term orientation.

To further explore the role of auxin transport, we tested the mutants of *PIN-FORMED 2* (*PIN2*), an auxin cellular exporter (Chen et al., 1998), and mutants of *AUXIN RESISTANT 1* (*AUX1*), an auxin cellular importer (Marchant et al., 1999). Since *pin2* and *aux1* mutants do not respond to gravity, to obtain a sufficient number of roots growing vertically in preparation for the electrotopism assay, we wrapped the sides and bottom of the nursery boxes with aluminum foil to induce negative root phototropism toward the bottom of the box (“Materials and methods”). The same setup was used to germinate WT plants to be compared with these to mutants.

Roots of *pin2* mutants (Figure 4, d) showed a significant response (paired Wilcoxon between the time-points 0 and 2 h, $P < 0.01$ and between the time-points 0 and 5 h, $P < 0.01$), but weaker than WT (t test between WT and *pin2* at 2 h, $P < 0.01$ and between WT and *pin2* at 5 h, $P < 0.01$) in the same conditions. Their angular velocity did not show an obvious decrease before reaching the target orientation, as with WT roots (Supplemental Figure S4, b).

Analogously, roots of *aux1* mutants (Figure 4, d) showed a significant early response (paired t test between the time-points 0 and 2 h, $P < 0.01$), but weaker than WT (t test between WT and *pin2* at 2 h, $P < 0.01$; t test between WT and *pin2* at 5 h, $P < 0.01$) in the same conditions. Interestingly, *aux1* roots on average failed to maintain their

orientation for a longer period (paired *t* test between the time-points 0 and 5 h, $P = 0.051$). Moreover, their angular velocity on average decreased while approaching the final orientation, as with WT roots (Supplemental Figure S4, b).

Taken together, these results suggest that although auxin transport seems to play a role in maintaining a sustained response to the electric field, it is not necessary for triggering early electrotropism.

Cytokinin biosynthesis is necessary for electrotropism

Given our results suggesting a limited role for auxin during electrotropism, we wondered which other plant hormones might be involved instead. Root hydrotropism, or the growth toward a high concentration of water, was also previously shown to be largely independent of auxin distribution in *Arabidopsis* (Shkolnik et al., 2016), while it requires biosynthesis and asymmetric distribution of cytokinin (Chang et al., 2019). Drawing an analogy with hydrotropism, we considered the possibility that electrotropism might act through cytokinin as well.

To test this hypothesis, we analyzed root electrotropism in triple mutants of *ARABIDOPSIS THALIANA* ISOPENTENYLTRANSFERASEs (*AtIPTs*), a family of adenosine phosphate-isopentenyltransferases required for the first step of isoprenoid cytokinin biosynthesis (Miyawaki et al., 2006; Kamada-Nobusada and Sakakibara, 2009). Within the tested mutants, although a high degree of redundancy is expected among the *AtIPTs*, we found two distinct behaviors: the triple mutants *atipt1,3,5* and *atipt3,5,7* both responded strongly to the electric field (Figure 5, a) (*t* test between 1.5 and 0 V/cm at 5 h, $P < 0.001$ in both cases), while the triple mutants *atipt1,3,7* and *atipt1,5,7* responded well in the first 2 h of exposure (Figure 5, b, left) (*t* test between 1.5 and 0 V/cm at 2 h, $P < 0.001$ for both mutants) but showed a much weaker, although still significant, response at 5 h (Figure 5, b, right) (*t* test between 1.5 and 0 V/cm at 5 h, $P < 0.01$ for *atipt1,5,7* and $P < 0.001$ for *atipt1,3,7*; *t* test between WT and mutant both at 1.5 V/cm at 5 h, $P < 0.001$ for *atipt1,5,7* and $P < 0.01$ for *atipt1,3,7*). These results suggest that cytokinin biosynthesis is in part required for long-term root electrotropism, and that for this phenotype *AtIPT1* and *AtIPT7* dominate their family in a redundant way (the response is the weakest when both are mutated).

To confirm the role of cytokinin, we also tested the requirement for CYTOCHROME P450, (*CYP735A1*), a cytochrome P450 monooxygenase enzyme acting downstream of *AtIPTs* and necessary for the biosynthesis of the trans-zeatin (*tZ*) variation of cytokinin (Takei et al., 2004). Interestingly, roots of *cyp735a1* mutants completely failed to respond to the electric field (Figure 5, c), with tip orientations indistinguishable from that of WT roots not exposed to the field (*t* test between *cyp735a1* exposed to 1.5 V/cm and WT not exposed at 5 h, $P = 0.748$). Crucially, this phenotype could be rescued the addition of the cytokinin *tZ* to the medium (Figure 5, c) (*t* test between *cyp735a1* + 10nM *tZ* at

1.5 and 0 V/cm, $P < 0.001$), while the same treatment did not affect WT response (Figure 5, c).

Taken together, these results indicate that cytokinin is necessary for electrotropism in *Arabidopsis* roots.

To further investigate a possible parallel between the molecular pathways involved in electrotropism and hydrotropism, we tested mutants of *MIZU-KUSSEIN1* (*MIZ1*), which is necessary for hydrotropism (Kobayashi et al., 2007) and its functional cytokinin asymmetric distribution in roots (Chang et al., 2019). Translational fusion reporters have shown *MIZ1* localization in the lateral root cap and the cortex of meristem and elongation zone (Dietrich et al., 2017): although the root tip is not necessary for hydrotropic response (Dietrich et al., 2017), this requires *MIZ1* in the transition zone (Dietrich et al., 2017).

When we exposed roots of *miz1* mutants to 1.5 V/cm (Figure 6) they showed an unperturbed electrotropic response in the first 2 h (Wilcoxon test between *miz1* and WT at 2 h, $P = 0.859$) and perhaps a weakened response at 5 h, although with only a weak statistical significance (*t* test between *miz1* and WT at 5 h, $P = 0.033$), indicating that *MIZ1* is not necessary for early root electrotropism.

Taken together, these surprising results indicate that cytokinin plays an important role in root electrotropism, but that the underlying molecular pathway differs early on from that of hydrotropism.

Discussion

The capability of plant roots to sense and combine numerous physical and chemical signals in soil is quite extraordinary, notably in the absence of a centralized processing system. The more we understand about the physical and molecular mechanism behind the various root tropisms, the closer we will get to a complete understanding of signal integration in plants. In this work, we focused on the little-studied phenomenon of root electrotropism and present a quantitative characterization in the flowering plant model system *A. thaliana*.

A non-trivial observation from this work is that plant roots respond to weak (order of 1 V/cm and 100 μ A) external electric fields and currents in a progressive way, with an increasingly stronger tendency to align with the field as the field and current intensities increase. This is interesting because it reveals a sophisticated way to discriminate between highly charged particles (e.g. ions, micro-organisms, and other plant roots) and weakly charged ones. At the same time, the absence of overshooting also points to a mechanism that perhaps can be modeled along the lines of a proportional–integral–derivative control system (Chevalier et al., 2019). Moreover, we show that the kinetics (response curve) of root electrotropism follows a power-law with exponents similar to those that have been traditionally measured in physiological responses to external stimuli in animal systems (Stevens, 1970): our results suggest that a power-law response to external stimuli might be a universal feature across life kingdoms, and that it does not require a nervous system. Moreover, it

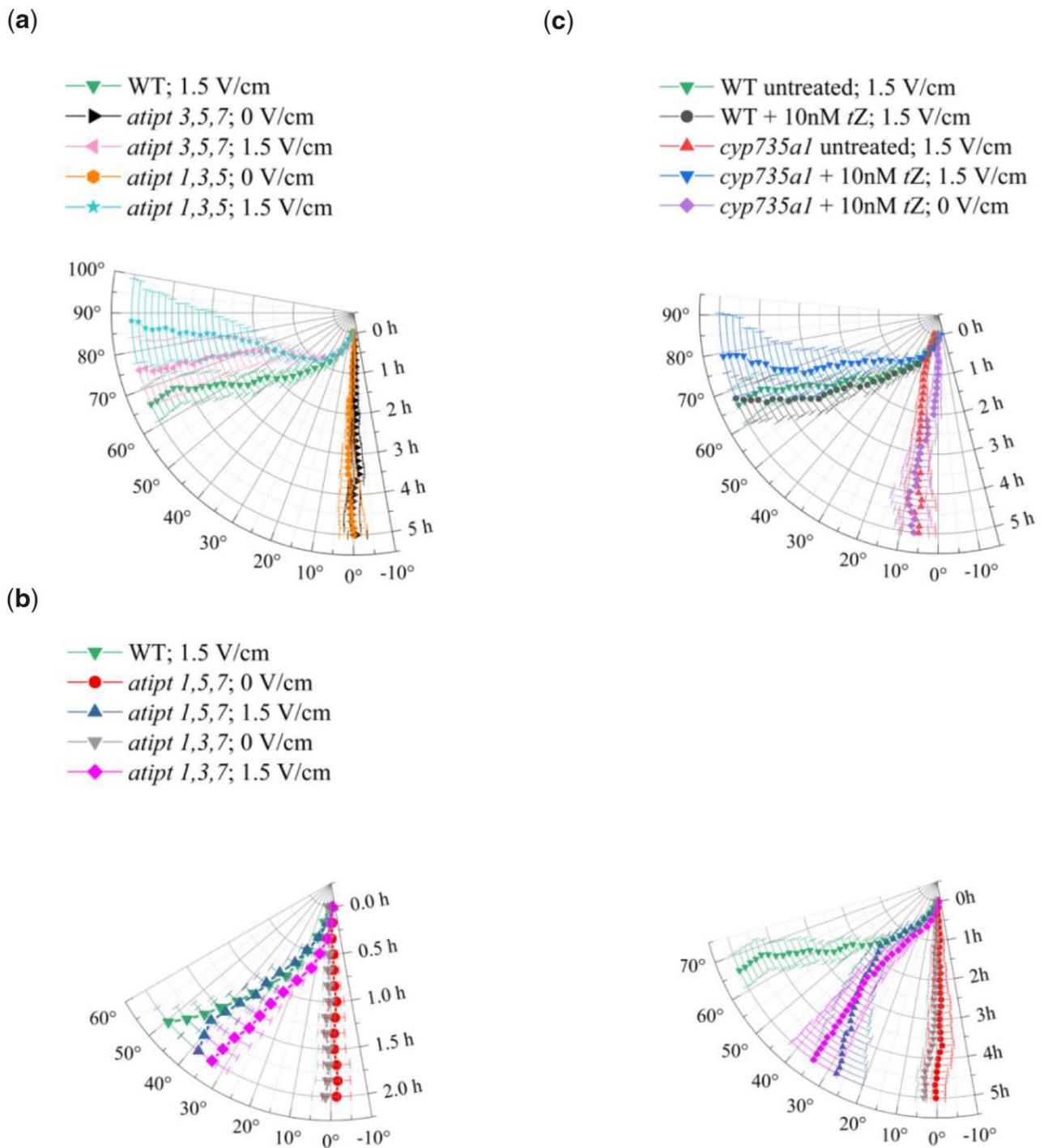


Figure 5 Cytokinin biosynthesis. Polar plots of the average root tip orientation relative to the gravity vector, with time on the radial axis and orientation angle on the circumferential axis: a, *atipt* triple mutants with strong electrotopism response; *atipt*3,5,7 at 0 V/cm, $N = 10$; *atipt*3,5,7 at 1.5 V/cm, $N = 15$; *atipt*1,3,5 at 0 V/cm, $N = 10$; *atipt*1,3,5 at 1.5 V/cm, $N = 15$. b, *atipt* triple mutants with weak electrotopism response; the same data are presented for the first 2 h (left panel) and for the full 5 h (right panel); *atipt*1,5,7 at 0 V/cm, $N = 10$; *atipt*1,5,7 at 1.5 V/cm, $N = 14$; *atipt*1,3,7 at 0 V/cm, $N = 10$; *atipt*1,3,7 at 1.5 V/cm, $N = 14$. c, *cyp735a1* mutant; untreated, $N = 20$; treated at 0 V/cm, $N = 14$; treated at 1.5 V/cm, $N = 13$; WT treated, $N = 14$; WT untreated, $N = 21$. Error bars, s.e.m.

might reveal constraints on the genetic architecture of the underlying sensory system (Adler et al., 2014).

A second, perhaps unexpected, result from this work is the identification of two regions in *Arabidopsis* roots required for the detection of the field: the section between

roughly 400 and 500 μm from the tip is necessary for the early detection (within 2 h from exposure), while the section between roughly 300 and 400 μm is necessary for a prolonged detection (up to 5 h from exposure). Interestingly, these sections seem to correspond to the well-characterized

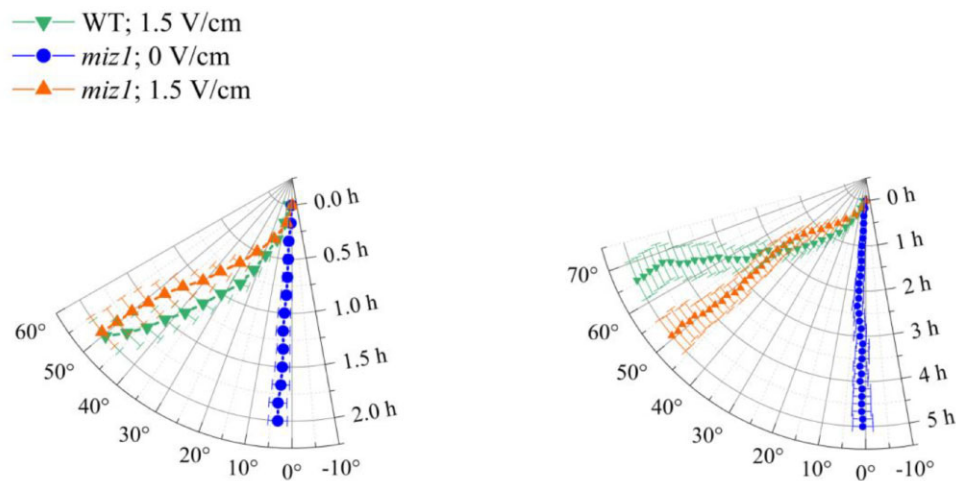


Figure 6 *miz1* is electrotopic. Polar plots of the average root tip orientation in *miz1* mutant (0 V/cm, $N = 10$; 1.5 V/cm, $N = 9$) relative to the gravity vector, with time on the radial axis and orientation angle on the circumferential axis. The same data are presented for the first 2 h (left panel) and for the full 5 h (right panel). WT, $N = 21$. Error bars, s.e.m.

anatomical transition zone, between the meristem and the elongation zone in roots, which has been previously involved in root sensing (Muthert et al., 2020). In future works, it will be crucial to discern whether the electrotopism mechanism depends on a relatively large region like the transition zone or if it can be narrowed to a more specific cell population therein.

Finally, we present evidence against the assumption that auxin asymmetric distribution is required for electrotopism in *Arabidopsis*, similarly to what was found for hydrotropism (Shkolnik et al., 2016) and phototropism (Kimura et al., 2018). Instead, we show that cytokinin is required for a full electrotopic response, although its response-specific regulation seems to act through a different pathway than the one established for hydrotropism.

Overall, our results show that root electrotopism requires a sensing mechanism likely localized in the transition zone, and a limited role for auxin but an important role for cytokinin. Cytokinin could be involved in a signaling or regulatory mechanism in the transition zone, in an actuator mechanism (tissue bending) in the elongation zone, or both.

Cytokinins have been shown to regulate root meristem activity and size by controlling cell proliferation (Beemster and Baskin, 2000) and the developmental progression from proliferation to elongation in the transition zone (Ioio et al., 2007). It has been suggested that root bending in hydrotropism is based on asymmetric distribution of cytokinin in the meristem to induce asymmetric cell proliferation (Chang et al., 2019). Although in this work we don't present data on cell proliferation and we cannot rule out a role for it, this seems an unlikely mechanism for electrotopism because roots without meristem (a 400- μm segment cut from the tip) still respond to the electric field, suggesting that cell proliferation does not play a major role in this tropic response. An alternative mode of action for cytokinins during electrotopism could be based on its regulatory action in

the transition zone, where an asymmetric delay in elongation would result in root bending. Although we have shown that *MIZ1* is not required for root electrotopism, it is still possible that a *MIZ1*-independent mechanism could generate an asymmetry in cytokinin distribution in the transition zone. These hypotheses will need to be tested in future work.

More recent studies have also shown that cytokinins participate in stress response through regulation of downstream factors and crosstalk with other hormones (Li et al., 2021; Wu et al., 2021). This signaling role could be relevant during electrotopism, especially since the transition zone has often been associated with signal integration in the root (Baluška et al., 2010).

Future work on root electrotopism should focus on testing these hypotheses regarding the role of cytokinin and on illuminating the still unknown molecular mechanism involved in sensing an electric field or current.

Materials and methods

Plant material

WT and mutant *Arabidopsis* (*A. thaliana*) plants were all from the Columbia (Col-0) ecotype; the following mutant alleles were used: *aux1-7* (NASC id 9583) for *aux1*; *eir1-1* (NASC id 8058) for *pin2*; SALK_093028C (NASC id N654306) for *cyp735a1*, *miz1-1* for *miz1* (courtesy of Prof. A. Kobayashi); *atipt* triple mutants as previously described with *atipt1-1*, *atipt3-2*, *atipt5-2*, *atipt7-1* (Miyawaki et al., 2006) (courtesy of Prof. O. Leyser).

The fluorescent line *WAVE131Y* is expressing *pUBQ10::WAVE131:YFP* (NASC id N781535); the fluorescent line *R2D2* is expressing *RPS5A-mDII-ntdTomato*, *RPS5A-DII-n3xVenus* (courtesy of Dr Teva Vernoux).

Seeds were imbibed in water and kept in the dark for 2 d at 4°C, to synchronize germination. All seeds were surface sterilized using 50% (v/v) Haychlor bleach and 0.0005% (v/v)

Triton X-100 for 3 min and then rinsed six times with sterilized milliQ water. Seed germination protocols are described in the experiment-specific “Materials and methods” sections below. Unless otherwise specified, all experiments were conducted with primary roots of seedlings 5–8 d post-germination, with roots approximately of the same length to be in the field of view of the V-box camera.

Electrotropism assay (V-box)

Seeds were sown individually inside PCR tubes filled with $1 \times$ MS gel medium: 0.44% (w/v) Murashige and Skoog (MS) Basal medium (Sigma–Aldrich, M5519), 0.5% (w/v) sucrose, 0.05% (w/v) MES hydrate (Sigma–Aldrich M8250), 0.8% (w/v) agar (Sigma–Aldrich 05040), and pH adjusted to 5.7 with Tris–HCl (Fisher–Scientific 10205100). The PCR tubes had their end cut out to allow the root to grow through and placed in a 3D-printed (Ultimaker 2+) holder inserted in a Magenta box (Sigma–Aldrich V8380). The Magenta box was filled with 150 mL of $1/500 \times$ MS liquid medium (0.00088% [w/v] MS Basal medium, 0.5% [w/v] sucrose, 0.05% [w/v] MES hydrate, pH adjusted to 5.7 with Tris–HCl) to reach the end of the PCR tubes. These germination, or “nursery,” boxes were placed in a growth chamber at 22°C, with a 16-h/8-h light/dark photoperiod and light intensity $120 \mu\text{mol m}^{-2} \text{s}^{-1}$.

In preparation for the electrotropism assay, each PCR tube containing a single seedling was transferred to a modified 3D-printed holder in a Magenta box filled with $1/500 \times$ MS liquid medium. The modified module consisted of a main body with five holes for the PCR tubes containing the seedlings and two side clips to position the electrodes consisting of platinum–iridium (Platinum:Iridium = 80:20; Alfa Aesar 41805.FF) foils (Figure 1, a), which were connected to an external power supply. In this paper, we refer to the Magenta box and its holder as the “V-box.” In addition to the five holes for the plants, four extra holes were designed: two at each end of the front side to pump the medium out of the V-box right on top of the two electrodes and two on the back to pump the medium in, using a tubing system and peristaltic pumps (Verdeflex AU R2550030 RS1) to circulate the medium at a speed of 1 mL/s to and from a 2-L reservoir bottle (Extended Data Figure 1). This configuration was designed and tested to ensure a slow and symmetric flow of medium in the box, eliminating any biased effect of the flow on the roots, which was confirmed by the control experiments at 0 V/cm, performed with the pump circulating the medium at the same speed as in the exposure experiments. Crucially, between the V-box and the reservoir bottle, the tubings were immersed in a cooled water bath (Grant Instruments, LTDGG) maintained at the constant temperature of 19°C (Extended Data Figure 1), which was enough to maintain the medium inside the V-box at a constant 22°C, as measured. All electrotopism experiments were performed at constant illumination.

The electric field was generated with a power supply attached to the platinum–iridium foil electrodes that were immersed in the liquid medium in the V-box. Standard electric

wires were soldered on the top of two electrodes, always kept outside the liquid medium to avoid contaminants from the solder. The voltage was set constant on the power supply, while the current was measured independently with a multimeter in series.

In order to record the movement of the roots over time, a Raspberry Pi camera module V2 (913-2664) connected to a Raspberry Pi board module B+ (137-3331) was used. The Raspberry Pi was programmed to take a picture every 10 min, using the command *crontab* in the local Raspbian OS.

WT electrotopism assays (Figure 1) were performed with the following sample sizes *N* and number of replicates *R*: 0 V/cm, *N* = 10, *R* = 2; 0.5 V/cm, *N* = 9, *R* = 2; 1.0 V/cm, *N* = 8, *R* = 2; 1.5 V/cm, *N* = 21, *R* = 5; 2.0 V/cm, *N* = 18, *R* = 6; 2.5 V/cm, *N* = 20, *R* = 7; foil-wrapped and 1.5 V/cm (control for *pin2* and *aux1*), *N* = 15, *R* = 3.

Mutants electrotopism assays (Figures 4–6) were performed with the following sample sizes *N* and number of replicates *R*: *aux1* at 1.5 V/cm, *N* = 18, *R* = 4; *aux1* at 0 V/cm, *N* = 14, *R* = 3; *pin2* at 1.5 V/cm, *N* = 13, *R* = 4; *pin2* at 0 V/cm, *N* = 13, *R* = 3; *atipt3,5,7* at 1.5 V/cm, *N* = 15, *R* = 3; *atipt3,5,7* at 0 V/cm, *N* = 10, *R* = 2; *atipt1,3,5* at 1.5 V/cm, *N* = 15, *R* = 3; *atipt1,3,5* at 0 V/cm, *N* = 10, *R* = 2; *atipt1,5,7* at 1.5 V/cm, *N* = 14, *R* = 3; *atipt1,5,7* at 0 V/cm, *N* = 10, *R* = 2; *atipt1,3,7* at 1.5 V/cm, *N* = 14, *R* = 5; *atipt1,3,7* at 0 V/cm, *N* = 10, *R* = 2; *cyp735a1* at 1.5 V/cm, *N* = 20, *R* = 4; *miz1* at 1.5 V/cm, *N* = 9, *R* = 2; *miz1* at 0 V/cm, *N* = 10, *R* = 2.

The control for medium circulation efficiency (Supplemental Figure S2) was performed with the following sample sizes *N* and number of replicates *R*: 1.5 V/cm, *N* = 10, *R* = 2; 0 V/cm, *N* = 10, *R* = 2.

The experiment showing gravitropism after 2 h of electric field (Supplemental Figure S7) was performed with a sample size *N* = 10 and replicates *R* = 2.

High temperature treatment

WT Col-0 seeds were germinated and grown in the nursery boxes as described in the “Electrotropism Assay.” The boxes undergoing treatment were then immersed in a water bath set at 50°C, for 10 min. The PCR tubes containing the seedlings were then transferred to a V-box, exposed to an electric field of 2.0 V/cm for 5 h, and imaged, as described in the “Electrotropism assay.”

Electrotropism assays for treated roots were performed with the following sample sizes *N* and number of replicates *R*: 23°C, *N* = 18, *R* = 6; 50°C, *N* = 10, *R* = 2.

For the gravitropism control, seedlings were treated with high temperature as described above and then transferred on $1 \times$ MS agar plates, to complete the assay as described in the paragraph “Gravitropism Assay.”

Gravitropic assays for treated roots were performed with the following sample sizes *N* and number of replicates *R*: 23°C, *N* = 10, *R* = 2; 50°C, *N* = 9, *R* = 1).

Electrotropism on microscope (V-slide)

Seeds of the transgenic reporter line WAVE131Y (see “Plant Material”) were germinated on $1 \times$ MS agar medium (0.44%

MS Basal medium, 0.5% sucrose, 0.05% MES hydrate, pH adjusted to 5.7 with Tris–HCl, 0.8% agar) in square plates kept vertical in a growth chamber at 22°C, with a 16-h/8-h light/dark photoperiod.

At 2 d post-germination, the seedlings were mounted on the V-slide with 1/500× MS liquid medium (0.00088% MS Basal medium, 0.5% sucrose, 0.05% MES hydrate, pH adjusted to 5.7 with Tris–HCl). The V-slide was then connected to the medium perfusion system circulating the same 1/500× MS medium and the V-slide's electrodes were connected to the power supply (Votcraft PS-1302-D).

Imaging was performed on a Leica SP5 laser scanning confocal microscope with 20× air objective, while the liquid medium was circulated and the electric field maintained constant. Fluorophore was excited with the 514 nm Argon laser line and the emission collected with PMT detector at 524–570 nm. Images were collected at intervals of 2 min.

Root tip excisions

Seeds were germinated in nursery boxes as described.

Three days post-germination seedlings still in their PCR tubes, as previously described, were transferred to hard 1× MS agar medium (0.44% MS Basal medium, 0.5% sucrose, 0.05% MES hydrate, pH adjusted to 5.7 with Tris–HCl, 5.0% agar) where the roots were manually dissected using a dental needle (Sterican, 27G) under a dissecting microscope (Nikon SMZ1000) at 180× magnification, following the published protocol (Kral et al., 2016).

After root tip excision, the PCR tubes containing the seedlings were immediately moved into the V-box for the electrotopism assay.

Electrotropism assays on excised roots were performed with the following sample sizes *N* and number of replicates *R*: 125 μm, *N* = 16, *R* = 4; 300 μm, *N* = 7, *R* = 2; 400 μm, *N* = 10, *R* = 2; 500 μm, *N* = 10, *R* = 2; uncut at 0 V/cm, *N* = 10, *R* = 2; uncut at 1.5 V/cm, *N* = 21, *R* = 5.

R2D2 reporter

Seeds of the transgenic reporter line R2D2 (see “Plant Material”) were germinated in nursery boxes and at 3 d post-germination exposed to 1.0 V/cm for 30 min in V-boxes, as described in the “Electrotropism assay.” After exposure, R2D2 roots were quickly mounted on standard microscope slides with sterile deionized water and imaged using Leica SP5 laser scanning confocal microscope, with 63× water immersion objective.

R2D2 expresses two versions of a protein that forms a complex with auxin: DII-n3xVENUS, which is degraded within minutes upon binding with auxin; mDII-ntdTOMATO, which contains a modified, non-degradable, version of DII. Both of the proteins are localized in the nucleus. We followed the published protocol (Liao et al., 2015) to separately collect the emission from mDII-ntdTOMATO (Extended Data Figure 6, a) and DII-n3xVENUS (Extended Data Figure 6, b).

For each root, a mean background was defined as the average pixel intensity in the mDII channel of a 80 × 80 pixels corner of the field of view not occupied by the root. The

mean background was then subtracted from all pixel intensities in both channels (mDII and DII). We manually segmented with Fiji (Schindelin et al., 2012) the most visible cell nuclei in the epidermis of each root, both in the distal (12 roots in mock conditions and 16 roots exposed to the field) and in the proximal (11 roots in mock conditions and 13 roots exposed to the field) regions of the root tip, and quantified the average pixel intensity (corrected after background subtraction) for each segmented nucleus. Finally, we calculated the natural log of the ratio between the average mDII (non-degradable, auxin-independent) and DII (degradable, auxin-dependent) signals in each nucleus and mapped it on top of the root image (Extended Data Figure 6, d).

For each root, we calculated the average and standard deviation of these ratios, for epidermal nuclei facing the anode or the cathode (Figure 4, b).

Sample size as follows: exposed to E field and imaged in distal region, *N* = 16; exposed to E field and imaged in the proximal region, *N* = 13; not exposed to E field and imaged in the distal region, *N* = 24; not exposed to E field and imaged in the proximal region, *N* = 22.

NPA treatment

To find the minimum concentration of NPA that inhibits gravitropism, seeds were germinated on 1× MS agar medium (0.44% MS Basal medium, 0.5% sucrose, 0.05% MES hydrate, pH adjusted to 5.7 with Tris–HCl, 0.8% agar) and at 5–8 d post-germination were transferred for 3 h into cell culture dishes containing 5 mL of 1/500× MS liquid medium (0.00088% MS Basal medium, 0.5% sucrose, 0.05% MES hydrate, pH adjusted to 5.7 with Tris–HCl) plus NPA at 0.1, 1.0, and 10 μM.

To quantify the effect of NPA on electrotopism, after being treated with a concentration of 10 μM NPA for 3 h as described above, the seedlings were transferred inside a V-box and exposed to a 1.5 V/cm electric field as described in the “Electrotropism Assay.” Both the V-box and the reservoir bottle contained 10 μM NPA throughout the experiment.

Sample sizes *N* and number of replicates *R* were the following: untreated, *N* = 21, *R* = 5; 10 μM NPA treated, *N* = 21, *R* = 5.

Cytokinin treatment

Both the 1× MS agar medium (0.44% MS Basal medium, 0.5% sucrose, 0.05% MES hydrate, pH adjusted to 5.7 with Tris–HCl, 0.8% agar) contained in the PCR tubes, and the 1/500× MS liquid medium (0.00088% MS Basal medium, 0.5% sucrose, 0.05% MES hydrate, pH adjusted to 5.7 with Tris–HCl) in the nurseries, were supplemented with 10 nM trans-zeatin (Sigma–Aldrich Z0876) as previously suggested (Miyawaki et al., 2006). Still in their PCR tubes, seedlings were transferred into V-boxes, filled with 1/500× MS liquid medium supplied with 10 nM trans-zeatin to conduct the electrotopism experiments.

Sample sizes *N* and number of replicates *R* were the following: WT + tZ, *N* = 14, *R* = 3; *cyp735a1* + tZ at 1.5 V/cm, *N* = 13, *R* = 3; *cyp735a1* + tZ at 0 V/cm, *N* = 14, *R* = 3.

Gravitropism assay

In the high-temperature experiment, after the treatment the seedlings were transferred onto $1 \times$ MS square agar plates (0.44% MS Basal medium, 0.5% sucrose, 0.05% MES hydrate, pH adjusted to 5.7 with Tris–HCl, 0.8% agar).

In the NPA experiment, after the treatment the seedlings were transferred onto $1/500 \times$ MS square agar plates (0.00088% MS Basal medium, 0.5% sucrose, 0.05% MES hydrate, pH adjusted to 5.7 with Tris–HCl, 0.8% agar) containing the desired concentration of NPA.

In both cases, the plates were moved to a growth room (22°C, 16-h/8-h light/dark photoperiod), rotated by 90 degrees to position the roots in a horizontal orientation, and monitored for root gravitropic response.

Statistical analysis

When comparing two samples of measurements, each distribution was first checked for normality with the Shapiro–Wilk test with alpha-level = 0.05. Normal distributions were tested with the two-tails Student's *t* test without assuming equal variances (Welch two-sample *t* test); if one of the two distributions was not normal, the non-parametric Mann–Whitney *U* (Wilcoxon) test was used. Unless stated otherwise, all comparisons were performed assuming independence (unpaired test). All statistical tests were performed with R.

Accession numbers

Sequence data from this article can be found in TAIR (www.arabidopsis.org) under accession numbers: *AUX1*, AT2G38120; *PIN2*, AT5G57090; *CYP735A1*, AT5G38450; *MIZ1*, AT2G41660; *ATIPT1*, AT1G68460; *ATIPT3*, AT3G63110; *ATIPT5*, AT5G19040; and *ATIPT7*, AT3G23630.

Supplemental data

The following materials are available in the online version of this article.

Supplemental Figure S1. V-box setup.

Supplemental Figure S2. V-box characterization.

Supplemental Figure S3. Live versus dead root.

Supplemental Figure S4. Velocity of electrotopism response.

Supplemental Figure S5. V-slide setup.

Supplemental Figure S6. Root meristem is not damaged.

Supplemental Figure S7. Roots exposed to the electric field are still gravitropic.

Acknowledgments

We thank T. Vernoux for providing *R2D2* seeds; O. Leyser for providing *atipt* triple mutant seeds; A. Kobayashi and Tohoku University for providing *miz1-1* seeds; A. Guyon, O. Kranse, C. Keyzor, and C.D. Livesey-Clare for generous technical help; and M. Levin and I. Bordeu for critical discussions at various stages of the project.

Funding

This work was partly supported by the Biotechnology and Biological Sciences Research Council (BBSRC) Impact

Acceleration Account grant BB/S506667/1 and the Allen Discovery Center at Tufts University. N.K. was supported by the BBSRC Doctoral Training Partnership (DTP) grant BB/M011178/1.

Conflict of interest statement. None declared.

References

- Adler M, Mayo A, Alon U (2014) Logarithmic and power law input–output relations in sensory systems with fold-change detection. *PLoS Comput Biol* **10**: e1003781
- Baluška F, Mancuso S, Volkmann D, Barlow PW (2010) Root apex transition zone: A signalling–response nexus in the root. *Trends Plant Sci* **15**: 402–408
- Beemster GTS, Baskin TI (2000) STUNTED PLANT 1 mediates effects of cytokinin, but not of auxin, on cell division and expansion in the root of *Arabidopsis*. *Plant Physiol* **124**: 1718–1727
- Chabert N, Ali OA, Achouak W (2015) All ecosystems potentially host electrogenic bacteria. *Bioelectrochemistry* **106**: 88–96
- Chang J, Li X, Fu W, Wang J, Yong Y, Shi H, Ding Z, Kui H, Gou X, He K, et al. (2019) Asymmetric distribution of cytokinins determines root hydrotropism in *Arabidopsis thaliana*. *Cell Res* **29**: 984–993
- Chen R, Hilson P, Sedbrook J, Rosen E, Caspar T, Masson PH (1998) The *Arabidopsis thaliana* AGRVITROPIC 1 gene encodes a component of the polar-auxin-transport efflux carrier. *Proc Natl Acad Sci USA* **95**: 15112–15117
- Chevalier M, Gómez-Schiavon M, Ng AH, El-Samad H (2019) Design and analysis of a proportional-integral-derivative controller with biological molecules. *Cell Syst* **9**: 338–353.e10
- Clarke D, Whitney H, Sutton G, Robert D (2013) Detection and learning of floral electric fields by bumblebees. *Science* **340**: 66–69
- Crampton WGR (2019) Electroreception, electrogenesis and electric signal evolution. *J Fish Biol* **95**: 92–134
- Dietrich D, Pang L, Kobayashi A, Fozard JA, Boudolf V, Bhosale R, Antoni R, Nguyen T, Hiratsuka S, Fujii N, et al. (2017) Root hydrotropism is controlled via a cortex-specific growth mechanism. *Nat Plants* **3**: 17057
- Elfving F (1882) Ueber eine Wirkung des galvanischen Stromes auf wachsende Wurzeln. *Bot Zeit* **40**: 257–264
- Ewart AJ, Bayliss JS (1905) On the nature of the galvanotropic irritability of roots. *Proc R Soc Lond Ser B* **77**: 63–66
- Geldner N, Déneraud-Tendon V, Hyman DL, Mayer U, Stierhof Y-D, Chory J (2009) Rapid, combinatorial analysis of membrane compartments in intact plants with a multicolor marker set. *Plant J* **59**: 169–178
- Gilroy S (2008) Plant tropisms. *Curr Biol* **18**: R275–R277
- Ioio RD, Linhares FS, Scacchi E, Casamitjana-Martinez E, Heidstra R, Costantino P, Sabatini S (2007) Cytokinins determine *Arabidopsis* root-meristem size by controlling cell differentiation. *Curr Biol* **17**: 678–682
- Ishikawa H, Evans ML (1990) Electrotopism of maize roots. Role of the root cap and relationship to gravitropism. *Plant Physiol* **94**: 913–918
- Kamada-Nobusada T, Sakakibara H (2009) Molecular basis for cytokinin biosynthesis. *Phytochemistry* **70**: 444–449
- Kimura T, Haga K, Shimizu-Mitao Y, Takebayashi Y, Kasahara H, Hayashi K-I, Kakimoto T, Sakai T (2018) Asymmetric auxin distribution is not required to establish root phototropism in *Arabidopsis*. *Plant Cell Physiol* **59**: 828–840
- Kobayashi A, Takahashi A, Kakimoto Y, Miyazawa Y, Fujii N, Higashitani A, Takahashi H (2007) A gene essential for hydrotropism in roots. *Proc Natl Acad Sci USA* **104**: 4724–4729
- Kral N, Ougolnikova AH, Sena G (2016) Externally imposed electric field enhances plant root tip regeneration. *Regeneration* **3**: 156–167

- Kutschera U, Briggs WR** (2012) Root phototropism: from dogma to the mechanism of blue light perception. *Planta* **235**: 443–452
- Li S-M, Zheng H-X, Zhang X-S, Sui N** (2021) Cytokinins as central regulators during plant growth and stress response. *Plant Cell Rep* **40**: 271–282
- Liao C-Y, Smet W, Brunoud G, Yoshida S, Vernoux T, Weijers D** (2015) Reporters for sensitive and quantitative measurement of auxin response. *Nat Methods* **12**: 207–210
- Marchant A, Kargul J, May ST, Muller P, Delbarre A, Perrot-Rechenmann C, Bennett MJ** (1999) AUX1 regulates root gravitropism in Arabidopsis by facilitating auxin uptake within root apical tissues. *EMBO J* **18**: 2066–2073
- Marcum H, Moore R** (1990) Influence of electrical fields and asymmetric application of mucilage on curvature of primary roots of *Zea mays*. *Am J Bot* **77**: 446
- McGillivray AM, Gow NAR** (1986) Applied electrical fields polarize the growth of mycelial fungi. *Microbiology* **132**: 2515–2525
- Miyawaki K, Tarkowski P, Matsumoto-Kitano M, Kato T, Sato S, Tarkowska D, Tabata S, Sandberg G, Kakimoto T** (2006) Roles of Arabidopsis ATP/ADP isopentenyltransferases and tRNA isopentenyltransferases in cytokinin biosynthesis. *Proc Natl Acad Sci USA* **103**: 16598–16603
- Miyazawa Y, Takahashi H** (2019) Molecular mechanisms mediating root hydrotropism: What we have observed since the rediscovery of hydrotropism. *J Plant Res* **133**: 3–14
- Muthert LWF, Izzo LG, Zanten M van, Aronne G** (2020) Root tropisms: Investigations on Earth and in space to unravel plant growth direction. *Front Plant Sci* **10**: 1807
- Navez AE** (1927) Galvanotropism of roots. *J Gen Physiol* **10**: 551–558
- Olitzki L** (1932) Electric charge of bacterial antigens. *J Immunol* **4**: 251–256
- Peters RC, Eeuwes LBM, Bretschneider F** (2007) On the electrode-tection threshold of aquatic vertebrates with ampullary or mucous gland electroreceptor organs. *Biol Rev* **82**: 361–373
- Pozdnyakov A, Pozdnyakova L** (2002) Electrical fields and soil properties. *Proceedings of 17th World Congress of Soil Science*. p. 1558
- Revil A, Naudet V, Nouzaret J, Pessel M** (2003) Principles of electrography applied to self-potential electrokinetic sources and hydrogeological applications. *Water Resour Res* **39**: 1–15
- Sabatini S, Beis D, Wolkenfelt H, Murfett J, Guilfoyle T, Malamy J, Benfey P, Leyser O, Bechtold N, Weisbeek P, et al.** (1999) An auxin-dependent distal organizer of pattern and polarity in the Arabidopsis root. *Cell* **99**: 463–472
- Schindelin J, Arganda-Carreras I, Frise E, Kaynig V, Longair M, Pietzsch T, Preibisch S, Rueden C, Saalfeld S, Schmid B, et al.** (2012) Fiji: An open-source platform for biological-image analysis. *Nat Methods* **9**: 676–682
- Shanley LJ, Walczysko P, Bain M, MacEwan DJ, Zhao M** (2006) Influx of extracellular Ca²⁺ is necessary for electroaxis in Dictyostelium. *J Cell Sci* **119**: 4741–4748
- Shkolnik D, Krieger G, Nuriel R, Fromm H** (2016) Hydrotropism: Root bending does not require auxin redistribution. *Mol Plant* **9**: 757–759
- Stevens SS** (1970) Neural events and the psychophysical law: Power functions like those that govern subjective magnitude show themselves in neuropsychic effects. *Science* **170**: 1043–1050
- Su S-H, Gibbs NM, Jancewicz AL, Masson PH** (2017) Molecular mechanisms of root gravitropism. *Curr Biol* **27**: R964–R972
- Sukul NC, Croll NA** (1978) Influence of potential difference and current on the electroaxis of *Caenorhabditis elegans*. *J Nematol* **10**: 314–7
- Sutton GP, Clarke D, Morley EL, Robert D** (2016) Mechanosensory hairs in bumblebees (*Bombus terrestris*) detect weak electric fields. *Proc Natl Acad Sci USA* **113**: 7261–7265
- Takamura T** (2006) Electrochemical potential around the plant root in relation to metabolism and growth acceleration. *In* AG Volkov, ed, *Plant Electrophysiology, Theory and Methods*. Springer, Berlin, pp 341–374
- Takei K, Yamaya T, Sakakibara H** (2004) Arabidopsis CYP735A1 and CYP735A2 encode cytokinin hydroxylases that catalyze the biosynthesis of trans-zeatin. *J Biol Chem* **279**: 41866–41872
- Thimann KV, Went FW** (1937) *Phytohormones*. The Macmillan Company, New York, USA. doi: 10.5962/bhl.title.5695
- Ward SH** (1990) *Geotechnical and environmental geophysics. In* Investigations in geophysics, Vol. 5. Soc. of Exploration Geophysicists, Tulsa, USA
- Wawrecki W, Zagórska-Marek B** (2007) Influence of a weak DC electric field on root meristem architecture. *Ann Bot* **100**: 791–796
- Wolverton C, Mullen JL, Ishikawa H, Evans ML** (2000) Two distinct regions of response drive differential growth in *Vigna* root electrotropism. *Plant Cell Environ* **23**: 1275–1280
- Wu Y, Liu H, Wang Q, Zhang G** (2021) Roles of cytokinins in root growth and abiotic stress response of *Arabidopsis thaliana*. *Plant Growth Regul* **94**: 1–10